ELSEVIER

Journal of Nuclear Materials 264 (1999) 333–353

journal of nuclear materials

The principal structural changes proceeding in Russian pressure vessel steels as a result of neutron irradiation, recovery annealing and re-irradiation

B.A. Gurovich *, E.A. Kuleshova, O.V. Lavrenchuk, K.E. Prikhodko, Ya.I. Shtrombakh

Russian Research Center Kurchatov Institute, Pl. Kurchatova, 123 182 Moscow, Russian Federation

Received 18 February 1998; accepted 3 June 1998

Abstract

A wide range of pressure vessel steels – in the initial state (i.e. unirradiated), after irradiation, recovery annealing and re-irradiation – have been studied using microstructural and fractographic methods. The analysis of the data has allowed quality explanations of the key features of radiation embrittlement (RE) in reactor pressure vessel steels (RPVS) and resulting from initial- and re-irradiation to be proposed, and also to justify the existing concepts concerning the mechanisms of RE.

1. Introduction

It is well established that radiation embrittlement (RE) in reactor pressure vessel steels (RPVS) is manifested as a shift in the temperature dependencies of the absorbed energy curves shift (transition curves) observed in impact tests, which results in an increase in ductile/brittle transition temperature (DBTT) [1,2]. The explanation for this RE can be found in the microstructural changes induced in the steels by neutron irradiation. These microstructural changes in irradiated RPVS have been investigated over a considerable period of time [3–5]. Different experimental methods have been applied, such as TEM, SEM, FEGSTEM, APFIM, SANS, SIMS and some others [6–10]. Despite this, the experimental data on radiation-induced structural changes in RPVS are still incomplete at the present time. It should be emphasized that the major fraction of such experimental data are those which can be used either for evaluations of hardening under irradiation (as a rule, the densities and sizes of copper–vacancy clusters, radiation defects etc.) or explanation of impurity influences (mainly, copper and, partly, phosphorus) on the RE coefficient. This situation is defined by the fact that until now radiation-induced hardening was considered as the principal factor controlling RE in the overwhelming majority of the studies [11].

But in review [12] it was demonstrated that radiation-induced hardening is not the only and, probably, not the principal cause of RE occurring in RPVS. Significant contribution to RE can be induced by intragranular segregation of impurities (e.g., phosphorus), forming at interface boundaries of precipitates (including the precipitates induced by irradiation, for instance, at copper-enriched precipitates or copper–vacancy clusters). Also an important contribution to RE occurring in RPVS can be ascribed to formation of grain-boundary segregation of impurities (e.g., phosphorus). In the above review, numerical evaluations of contributions to the total value of absorbed energy measured in impact tests from different components (elastic, surface, ductile) have been calculated. It was demonstrated in [12] that the peculiarities of the transition curves, which are typical of the steels possessing BCC crystal lattice, can be explained exclusively by the component of absorbed energy responsible for ductile deformation of the material (preceding fracture).

* Corresponding author. Tel.: +7-095 196 1701; fax: +7-095 196 9215; e-mail: guvovich@nw.oirtorm.net.kiae.su.

0022-3115/99/$ – see front matter
PII: S0022-3115(98)00455-3

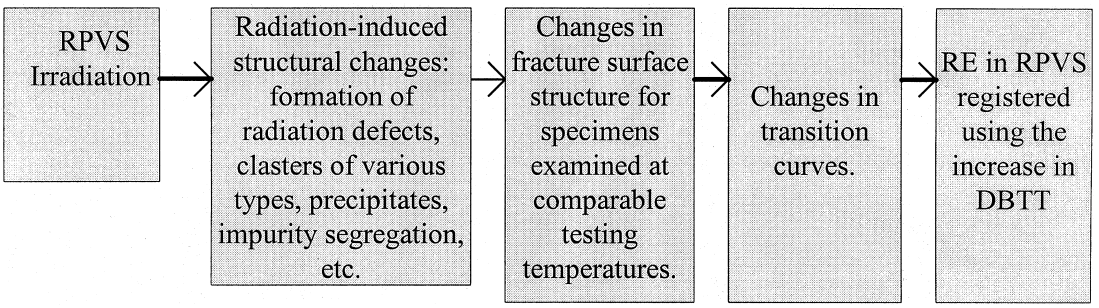

Fig. 1. The scheme of RE in RPVS.

In this connection, it would be reasonable to expect that fracture surfaces of Charpy specimens that have undergone testing at different or comparable temperatures, before and after irradiation, directly reflect information on the mechanisms responsible for RE occurring in RPVS. In general, final heat treatments applied to steels possessing BCC crystal lattice – in particular, RPVS – are, in the majority of cases, carefully chosen to avoid traces of temper brittleness. As a consequence, the fracture surfaces of unirradiated specimens from RPVS present different combinations of regions of ductile dimple fracture as well as cleavage and quasicleavage, but, as a rule, an absence of intergranular fracture [13]. In the simplest, idealized case, when RE occurring in steels is determined exclusively by matrix hardening, irradiation has not to induce new structural component types in fracture surfaces of Charpy specimens. However, in real cases, when RE in RPVS is caused of the simultaneous effect of several mechanisms – in particular, radiation-induced grain-boundary and intragranular impurity segregation, additional regions may appear in fractures of the specimens demonstrating the occurrence of brittle intergranular and ductile intergranular fracture type [12].

In general, the process of RE evolution, evaluated using the DBTT shift in transition curves, can be represented schematically as shown in Fig. 1.

Therefore, to reveal properly the mechanisms responsible for RE occurring in RPV materials, it is extremely important to compare the data obtained in fractographic studies (item 3 in Fig. 1) with the data obtained in studies that deliver information on the parameters indicated in item 2.

It appears unlikely that a comprehensive understanding of the mechanisms responsible for RE in RPVS can be achieved without structural studies applied to the same materials which have undergone recovery annealing and re-irradiation.

Based on the above rationale, microstructural and fractographic studies have been carried out on RPVS steels in initial (unirradiated) state, after irradiation, recovery annealing and re-irradiation. The objective of the investigations was the comparison of structural and fractographic data in order to elucidate the mechanisms governing RE in RPVS.

2. Experimental

The range of chemical compositions of the RPVS investigated is presented in Table 1.

After forging, base metals: 15Kh2MFA was austenized 1000°C – 10 h, oil cooling; tempering: 700°C – 16 h, air cooling; 15Kh2NMFAA was austenized at 920°C – 1 h, water cooling, aging 650°C, air cooling, aging 620°C – 25 h, aging 650°C – 20 h, furnace cooling to room temperature.

25Kh3NM is the base metal (experimental PWR) that was given the following heat treatment: 870–890°C,

Table 1
Chemical composition of investigated pressure vessel material

Steel type	W%									
	Si	Mn	P	S	Cu	Ni	Cr	Mo	C	V
15Kh2MFA	0.27	0.39	0.011	0.012	0.19	2.52	0.64	0.13	0.25	
	0.37	0.48	0.016	0.018	0.14	0.27	3.00	0.71	0.18	0.31
SV-10KhMFT	0.15	0.97	0.029	0.012	0.15	0.09	1.37	0.43	0.05	0.19
	0.35	1.03	0.036	0.013	0.21	0.29	1.58	0.50	0.07	0.23
15Kh2NMFAA	0.23	0.42	0.010	0.008	0.09	1.25	2.14	0.59	0.16	0.10
25Kh2NMFAA	0.44	0.49	0.024	0.018	0.10	1.02	3.03	0.40	0.23	–

air cooling to 700–800°C, oil quenching, tempering at 620–670°C and furnace cooling.

Post weld heat treatment for the weld metal (SV-10KhMFT): holding 15 h at 665°C, furnace cooling to 300°C, then air cooling.

Embrittlement of the specimens after irradiation was assessed from the DBTT shift and the decrease of the upper shelf energy in impact tests on Charpy V-notch specimens.

DBTT values were determined from impact testing carried out in accordance with ASTM standards.

Fractographic examinations were carried out on halves of Charpy specimens, which were stored under vacuum after testing, in order to preserve the fracture surfaces.

The fracture surfaces were investigated using an X-ray microbeam SXR-50 – radioactive version (''Cameca'') that was installed in a shielded chamber. The images of the fractures were obtained with secondary electrons at an accelerating voltage 20 kV and a probe current 0.8 nA, with magnifications in the range 50–3500 times. The fractions of different types of fracture (ductile, brittle intergranular, ductile intergranular, cleavage and quasicleavage) in the total fracture surface after tests at different temperatures were evaluated using the Glagolev method [14]. The absolute error of measurements at 95% confidence level did not exceed 5%. Testing temperatures for each material corresponded to upper shelf (US), DBTT and lower shelf (LS) in the temperature dependence of absorbed energy.

An electron microscope type TEMSCAN-200CX was used for transmission electron microscopic (TEM) studies at an accelerating voltage 200 kV. In those regions where the densities of both radiation defects and precipitates were determined, the specimen thickness was simultaneously determined using the Convergent Beam Electron Diffraction method [15], giving an error less than 5%.

Specimens for TEM studies were cut from the halves of fractured Charpy specimens. Further machining of the specimens consisted in electrolytic polishing carried out using a ''Struers'' electropolisher just before electron-microscopic studies. The composition of the electrolyte was as follows: 10% of $HClO_4$ and 90% of methanol at −60° to −75°C.

The chemical composition of grain boundaries was studied by the methods of Secondary-Ion Mass-Spectroscopy (SIMS) and Auger-electron spectroscopy using Escalab-5 (VG, UK) designed for combined analysis of the surface. Cylindrical specimens made from steel pieces of 25 mm length and 4 mm in diameter with a ring notch 1 mm depth and a notch root radius of 0.1 mm were tested. The specimens were then brittle fractured using impact bend at −170°C in a vacuum of 10^{-9} Torr inside the spectrometer chamber. The data cited have been obtained for unoxidized fractures. The depth analyzed was 2.0–2.5 nm. Semiquantitative comparative analysis of alloy and impurity content was obtained by determination of the following ratio: the amplitude of phosphorus Auger peak (120 eV) to the amplitude of iron Auger peak (703 eV) [16]. Semiquantitative evaluation was derived from experimental data averaged over 7–10 boundaries (facets) for grains of different orientations to reduce any influence of this factor on the data.

3. Results

3.1. Examination of fracture surfaces

Table 2 shows the data typical of fractographic studies carried out with specimens from RPVS in the initial state, after irradiation in different conditions, recovery annealing and re-irradiation. These data permit to formulate the series of general regularities concerning the fracture surface structure typical of the specimens from RPVS in different conditions.

1. In the initial unirradiated state, fracture proceeds almost exclusively by a transcrystalline mode over the whole range of impact test temperatures – LS through US – for all steels examined. [1] Moreover, in the regime of US temperatures, 100% of fracture surfaces in the specimens exhibit ductile, dimple type fracture (Fig. 2). As the testing temperature decreases, the fraction of the regions with ductile type of fracture in the fracture surfaces decreases and regions with cleavage and quasicleavage fracture type appear (Fig. 3). Their fraction increases with approach to LS. In LS vicinity, the regions with ductile type fracture are practically not observed. Quantitative processing of fractographic data shows that normalized values of the absorbed energy (A/A_{US}) correlates with the fraction of regions with ductile type fracture in the whole fracture surface over the whole range of impact testing temperatures [13].

2. Irradiation of RPVS under conditions characteristic of RPV operation leads to significant changes in fractography of Charpy specimens at comparable test temperatures. For instance, in the fractures of specimens tested within the US interval, in addition to regions with ductile, dimple fracture type, ductile intergranular regions appear (Fig. 4). As known, this type of fracture can appear in the case of precipitates located along grain boundaries to which interfaces phosphorus segregates. Ductile intergranular fraction of the total fracture sur-

[1] Under conditions that the final heat treatment was performed correctly and enabled temper brittleness to be avoided.

Table 2
Summary data of fractographic analysis results for investigated Charpy specimens

N	Material, wt%	Specimen types	NPP unit	Fluence, $\times 10^{23}$ n/m^2	Condition	Test temp., °C	DBTT (T_k), °C	Absorb. energy, J	Point on the curve KCV-T	Fraction of different fracture modes, %				
										Ductile	Quasi-cleavage	Cleavage	Inter-granular	Ductile inter-granular
1	2	3	4	5	6	7	8	9	10	11	12	13	14	15
1	25Kh3NM	BM	Cover from		unirrad.,	−150		5.4	LS	–	35	–	65	–
2	P = 0.018	Charpy	experimental	–	heat influence	−35	−22	46	DBT	10	5	5	65	15
3	Cu = 0.10		PWR		−60 000 h.	100		191	US	85	–	–	–	15
4	25Kh3NM	BM	Trepan from			0		18	LS	10	15	10	65	–
5	P = 0.018	Charpy	experimental	1.6	irrad.	113	107	47	DBT	35	10	–	45	10
6	Cu = 0.10		PWR			200		108	US	90	–	–	–	10
7	25Kh3NM	BM	Trepan from	5.05		23		5	LS	10	20	–	70	–
8	P = 0.018	Charpy	experimental	3.7	irrad.	175	168	40	DBT	40	5	5	40	10
9	Cu = 0.10		PWR	3.7		225		90	US	90	–	–	–	10
10	Sv−10KhMFT	WM	Trepan from			−50		4.2	LS	5	95	–	–	n/d
11	P = 0.034	Charpy	WWER-440	6.5	irrad.	125	145	43	DBT	60	40	–	–	n/d
12	Cu = 0.155					213		72	US	90	10	–	–	n/d
13	Sv-10KhMFT	WM	Trepan from			−50		1.4	LS	10	70	15	5	n/d
14	P = 0.034	subsize	WWER-440	6.5	irrad.	50	71	4.2	DBT	40	40	10	10	n/d
15	Cu = 0.155	Charpy				250		11.5	US	100	–	–	–	n/d
16	Sv−10KhMFT	WM	Trepan from		irrad. +	−25		10	LS	15	65	20	–	n/d
17	P = 0.034	Charpy	WWER-440	6.5	annealed	50	48	65	DBT	75	15	10	–	n/d
18	Cu = 0.155				475°C, 150 h	150		90	US	100	–	–	–	n/d
19	15Kh2MFA	BM	Templet from			−100		0.4	LS	5	30	50	15	n/d
20	P = 0.017	subsize	WWER-440	9.2	irrad.	−25	−25	2.6	DBT	20	20	45	15	n/d
21	Cu = 0.17	Charpy				200		6.6	US	100	–	–	–	n/d
22	15Kh2MFA	BM	Templet from		irrad. +	−100		0.8	LS	5	80	–	15	n/d
23	P = 0.017	subsize	WWER-440	9.2	annealed	−60	−49	1.1	DBT	5	50	20	25	n/d
24	Cu = 0.17	Charpy			475°C, 150 h	200		6.0	US	100	–	–	–	n/d
25	Sv-10KhMFT	WM	Templet from			−50		0.4	LS	10	75	10	5	n/d
26	P = 0.0375	subsize	WWER-440	6.7	irrad.	150	91	8.2	DBT	80	10	5	5	n/d
27	Cu = 0.18	Charpy				250		9.6	US	100	–	–	–	n/d
28	Sv−10KhMFT	WM	Templet from		irrad. +	−50		1.5	LS	15	75	5	5	n/d
29	P = 0.0375	subsize	WWER-440	6.7	annealed	25	11	7.7	DBT	30	50	15	5	n/d
30	Cu = 0.18	Charpy			475°C, 150 h	250		14.4	US	100	–	–	–	n/d

Table 2 (Continued)

N	Material, wt%	Specimen types	NPP unit	Fluence, $\times 10^{23}$ n/m^2	Condition	Test temp., °C	DBTT (T_k), °C	Absorb. energy, J	Point on the curve KCV-T	Fraction of different fracture modes, %				
										Ductile	Quasi-cleavage	Cleavage	Inter-granular	Ductile inter-granular
1	2	3	4	5	6	7	8	9	10	11	12	13	14	15
31	Sv–10KhMFT	WM	Templet from		irrad. +	−50		2.9	LS	20	65	15	–	n/d
32	P = 0.0375	subsize	WWER-440	6.7	annealed	−37	−24	6.7	DBT	30	45	25	–	n/d
33	Cu = 0.18	Charpy			560°C, 2 h	150		15.2	US	90	5	5	–	n/d
34	15Kh2NMFAA	BM	Research			−100		3	LS	–	70	30	–	n/d
35	P = 0.009	Charpy	specimen	–	unirrad.	−25	−20	45	DBT	50	50	–	–	n/d
36	Cu = 0.09		WWER-1000			100		120	US	100	–	–	–	n/d
37	15Kh2NMFAA	BM	Research			−100		2.5	LS	–	65	20	15	n/d
38	P = 0.009	Charpy	specimen	5	irrad.	55	60	40	DBT	55	35	–	10	n/d
39	Cu = 0.09		WWER-1000			100		87	US	100	–	–	–	n/d
40	15Kh2NMFAA	BM	Research		irrad. +	−20		8.5	LS	–	70	–	30	n/d
41	P = 0.009	Charpy	specimen	5	anneal.	10	0	55	DBT	50	35	–	15	n/d
42	Cu = 0.09		WWER-1000		480°C, 50 h	80		100	US	80	20	–	–	n/d
43	Sv-10KhMFT	WM	Templet from			−125		0.26	LS	–	85	5	10	–
44	P = 0.047	subsize	WWER-440	0.5	reirrad.	40	54	5.01	DBT	35	45	5	5	10
45	Cu = 0.10	Charpy				225		13.83	US	75	5	–	5	15
46	Sv-10KhMFT	WM	Templet from		reirrad. +	−125		0.38	LS	–	75	15	10	–
47	P = 0.047	subsize	WWER-440	0.5	anneal.	40	27	7.32	DBT	45	25	15	10	5
48	Cu = 0.10	Charpy			475°C, 150 h	150		14.84	US	80	traces	traces	10	10
49	Sv-10KhMFT	WM	Templet from		irrad. +	−110		0.38	LS	–	90	10	traces	–
50	P = 0.047	subsize	WWER-440	0.5	anneal.	12	1	9.75	DBT	55	30	5	5	5
51	Cu = 0.10	Charpy			560°C, 2 h	150		16.36	US	95	–	–	–	5
52	Sv-0KhMFT	WM	Surveillance			−150		1.6	LS	–	65	35	–	–
53	P = 0.039	Charpy	samples	–	unirrad.	−12	10	41	DBT	35	40	25	–	–
54	Cu = 0.17		WWER-440			175		135	US	100	–	–	–	–
55	Sv-0KhMFT	WM	Surveillance			60		24.3	LS	30	60	10	–	–
56	P = 0.039	Charpy	samples	0.9	irrad.	100	100	43.9	DBT	60	35	5	–	–
57	Cu = 0.17		WWER-440			160		83.1	US	90	–	–	–	10
58	Sv-0KhMFT	WM	Surveillance		irrad. anneal.	0		10.2	LS	10	55	35	–	–
59	P = 0.039	Charpy	samples	0.9	470°C, 70 h	20	25	48.6	DBT	40	35	25	–	–
60	Cu = 0.17		WWER-440			100		137. 2	US	85	5	5	–	5

Table 2 (Continued)

N	Material, wt%	Specimen types	NPP unit	Fluence, $\times 10^{23}$ n/m^2	Condition	Test temp., °C	DBTT (T_k), °C	Absorb. energy, J	Point on the curve KCV-T	Fraction of different fracture modes, %				
										Ductile	Quasi-cleavage	Cleavage	Inter-granular	Ductile inter-granular
1	2	3	4	5	6	7	8	9	10	11	12	13	14	15
61	Sv-0KhMFT	WM	Surveillance			−50		5	LS	–	65	35	–	–
62	P = 0.039	Charpy	samples	0.9	reirrad.	60	85	51	DBT	55	30	15	–	–
63	Cu = 0.17		WWER-440			250		95	US	90	–	–	–	10

BM – Base Metal; WM – Weld Metal; LS – Lower Shelf; DBT – Ductile to Brittle Transition Region; US – Upper Shelf; n/d – not determined.

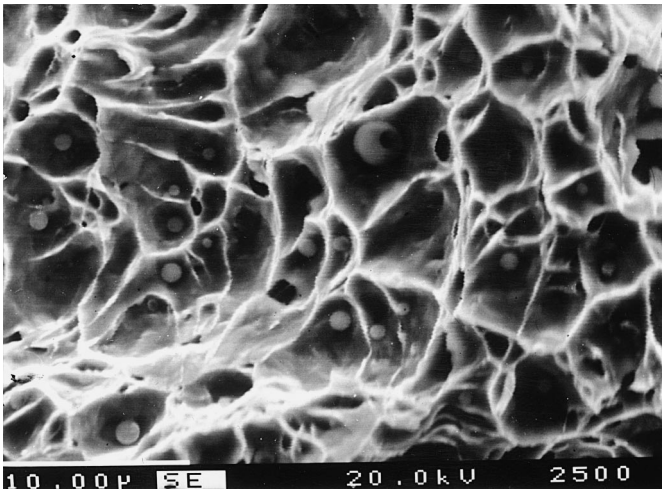

Fig. 2. Typical ductile dimple fracture (unirradiated base metal, $T_{test} = 100°C$).

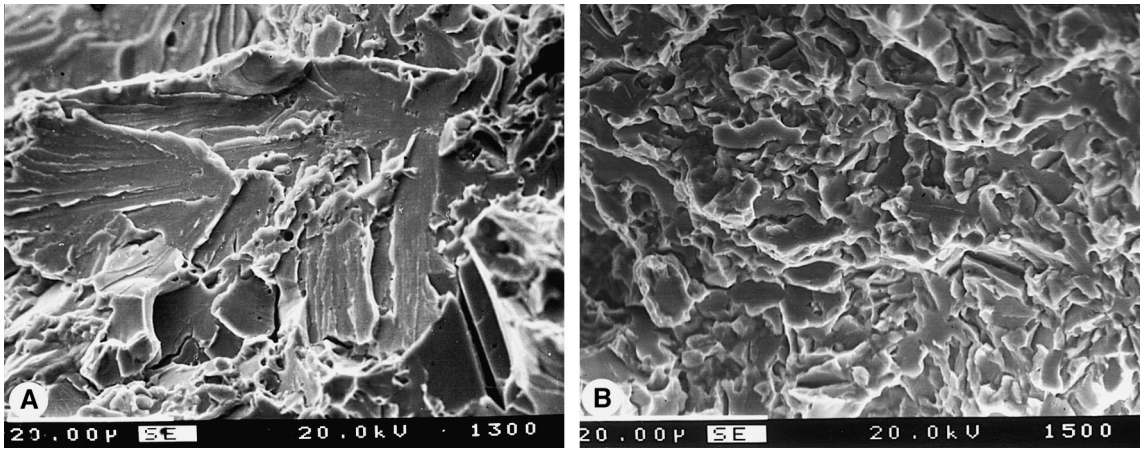

Fig. 3. Brittle transcrystalline fracture (irradiated base metal, $T_{test} = -100°C$): (A) cleavage; (B) quasicleavage.

face reaches 10–15% (Table 2, lines 1–9). [2] When the testing temperature is decreased to values close to the DBTT, then a significant decrease in the fraction of the regions with ductile and ductile intergranular fracture type is observed in the total fracture surface area (Table 2). In parallel with this phenomenon, it is observed the presence of considerable number of the regions where the fracture had occurred as a result of cleavage or quasicleavage (Table 2). It should be noted that in the base metal, irradiation induces the appearance of appreciable number of the regions with brittle intergranular fracture type (Fig. 5A). Usually, their fraction in the total fracture surface area constitutes ≈15–30% (Table 2, lines 19,20,22,23,37,40,41). But for some steel types this fraction can reach ≈70% (Table 2, lines 1–9). It should be emphasized that in fractures of full-size Charpy specimens made from irradiated WWER-440 weld metal (even, with phosphorus content reaching ≈0.05%) the regions with brittle intergranular fracture type is practically not observed (Table 2, lines 16–18, 31–33). On the other hand, due to the peculiarities of stress deformation state arising in impact tests (at comparable temperatures) with sub-size Charpy specimens made from the same materials, the appearance of

[2] Until 1996 the authors did not distinguish ductile intergranular component in fracture surfaces as a special type of fracture, when analyzing the data of fractographic studies. But latter part of those data had been revised and it was shown that this fracture type ought to be identified as a special fracture type. The regions of this fracture type are present in fractures of all examined specimens of irradiated steels tested over the interval DBTT through USE.

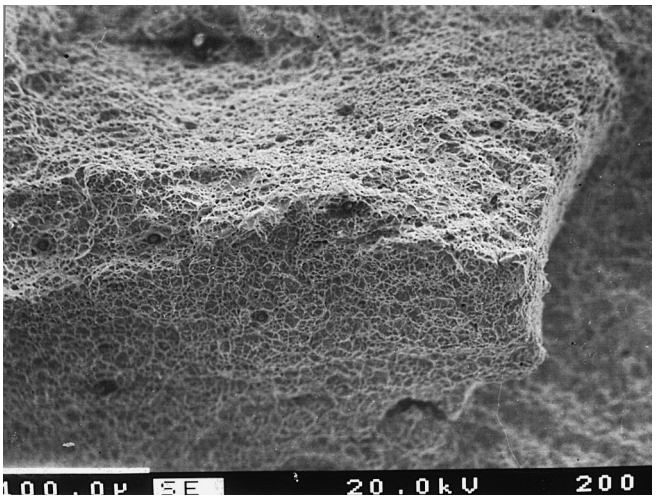

Fig. 4. Ductile intergranular fracture (irradiated weld metal, $T_{test} = 160°C$).

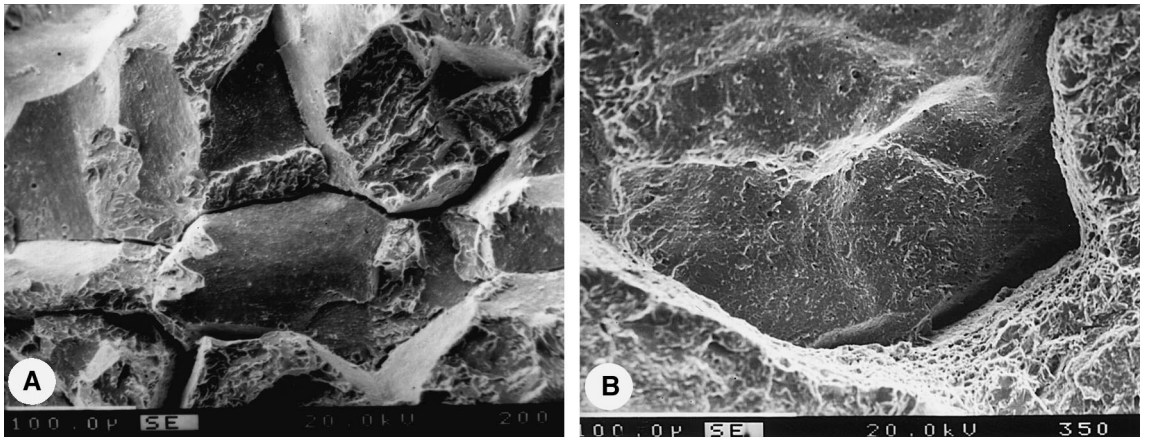

Fig. 5. Brittle intergranular fracture: (A) irradiated base metal ($P = 0.009\%$wt, $T_{test} = -100°C$); (B) sub-size Charpy specimen from irradiated weld metal ($P = 0.047\%$wt, $T_{test} = 150°C$).

the regions with the brittle fracture type are observed (Fig. 5(b)). Their fraction in total area of fracture surfaces can reach ≈5–15% (Table 2, lines 13,14,19,20, 25,26,28,29,43–48). It should be mentioned that an increased phosphorus content in the steel (≈0.04%) causes the appearance of a brittle intergranular component within the whole test temperature interval up to temperatures close to US (Table 2, lines 45,48) that is observed in fracture surfaces of sub-size Charpy specimens.

Further decrease in impact testing temperature to values corresponding to the LS, results in practically complete disappearance of the regions with ductile and ductile intergranular fracture type in the irradiated specimen fractures (Table 2). At the same time, sometimes some reduction in the fraction of the regions with intergranular fracture character occurs (in those materials where it had existed) in the total area of fracture surfaces (Table 2, lines 13,14,22,23). In contrast with the above situation, the fraction of the regions with cleavage and quasicleavage fracture type increases (Table 2).

Thus, comparative fractographic investigations of a wide range of RPVS (both base and weld metal) in the initial state and after irradiation have demonstrated that the principal characteristic feature of fracture surfaces of irradiated Charpy specimens is the transition from purely transcrystalline to mixed fracture type, in which brittle and/or ductile intergranular fracture may be present. Moreover, the higher the phosphorus content in the steel, the higher the temperature interval where the intergranular component appears and also the higher the fraction of this component in the fracture surface of a specimen made from one material type (base or weld).

3. Recovery annealing applied to irradiated RPVS leads to considerable changes occurring in fracture surfaces at comparable impact test temperatures. However, the degree and character of such changes depends on the annealing temperature.

(a) If the annealing temperature is ≈450–475°C and the duration of heat treatment does not exceed ≈150 h, then an appreciable decrease in the fraction of the regions with ductile intergranular fracture character in the total fracture surface area is observed (Table 2, compare lines 43–45 with 46–48 and 57 with 60). Simultaneously, the fraction of the regions with ductile fracture type grows by the appropriate value.

(b) This is important that in addition to the fact that recovery annealing at 450–475°C does not induce reduction in the fraction of the regions with brittle intergranular fracture type, in some cases it induces even its increase (Table 2, compare lines 19,20 with 22,23 and 37,38 with 40,41).

Recovery annealing at 560°C leads to subsequent reduction in the fraction of the regions with ductile intergranular fracture type in specimens (Table 2, compare lines 48 with 51). Besides, such annealing induces significant decrease in the fraction of the regions with brittle intergranular fracture type in the specimens (Table 2, compare lines 28,29 with 31,32 and 46–48 with 49–51).

4. Re-irradiation of the steels, which have previously undergone recovery annealing at 475°C, induces the repeated appearance of the regions with ductile intergranular fracture type in Charpy specimens tested at US and DBTT (Table 2, lines 44,45,63). It should be noted that, practically, re-irradiation does not change of the ductile intergranular and brittle intergranular fracture types in the total fracture surface, when compared with initial irradiation at the same conditions (Table 2, compare lines 57 with 63).

3.2. Microstructural studies using TEM methods

Table 3 demonstrates the data typical of electron-microscopic studies with RPVS – in the initial state, after irradiation in different conditions, recovery annealing and re-irradiation. These data enable the following series of general regularities concerning the character of radiation-induced structural changes occurring due to initial- and re-irradiation as well as recovery annealing to be identified.

1. The most important type of radiation-induced structural change in RPVS is the formation of radiation defects and two kinds of precipitates: disk- and round-shaped (Table 3). Radiation defects in steel are visible as "black dots" and dislocation loops with a zero contrast line (Fig. 6). The analysis of dark-field images obtained using different diffraction vectors shows that

Table 3
Data on densities and average sizes of radiation defects, disk-shaped and rounded precipitates in weld metal before irradiation, after irradiations and after recovery annealings

No	Condition	n_{loods}, × 10^{15} cm^{-3}	$\langle d\rangle_{\text{loods}}$, nm	n_{disk}, × 10^{15} cm^{-3}	$\langle d\rangle_{\text{disk}}$, nm	n_{rounded}, × 10^{15} cm^{-3}	$\langle d\rangle_{\text{rounded}}$, nm
Specimens from trepan of WWER-440 (P = 0.034%, Cu = 0.155%)							
1	unirradiated quasi-archive	–	–	0.5–0.6	20.4	–	–
2	irradiated F = 6.5 · 1 0^{23} m^{-2}	7–8	5	50–60	10.5	n/d [a]	n/d
3	irradiated + annealed 475°C, 150 h	–	–	3.5–4.0	13.5	n/d	n/d
4	irradiated + annealed 560°C, 2 h	–	–	0.7–0.9	20.5	n/d	n/d
5	irradiated F = 2.7 · 1 0^{23} m^{-2}	5–6	3	30–50	9.5	n/d	n/d
6	irradiated + annealed 475°C, 150 h	–	–	2.5–3.0	17.5	n/d	n/d
7	irradiated + annealed 560°C, 2 h	–	–	0.9–1.0	23.5	n/d	n/d
Specimens from templet of WWER-440 (P = 0.047%, Cu = 1.0%)							
8	unirradiated quasi-archive	–	–	0.5–0.6	20.4	–	–
9	reirradiated F = 0.5 · 1 0^{23} m^{-2}	0.9–1.0	4–5	2.0–3.0	11.5	500–700	2.0–3.0
10	reirradiated + annealed 475°C, 150 h	–	–	1.0–1.5	11.5	20–30	3.0–4.0
11	reirradiated + annealed 560°C, 2h	–	–	0.8–0.9	12.0	15–20	3.0–4.0
Surveillance samples from WWER-440 (P = 0.039%, Cu = 0.17%)							
12	unirradiated	–	–	0.7–0.8	22.8	–	–
13	irradiated F = 0.9 · 1 0^{23} m^{-2}	2–3	5–6	20–25	18.7	1700–2000	2.0–2.5
14	irradiated + annealed 470°C, 70h	–	–	2.5–3.0	25.6	40–50	3.0–4.0
15	reirradiated F = 0.9 · 1 0^{23} m^{-2}	1.5–2.0	5–6	10–15	23.3	400–500	3.5–4.5

[a] Not determined.

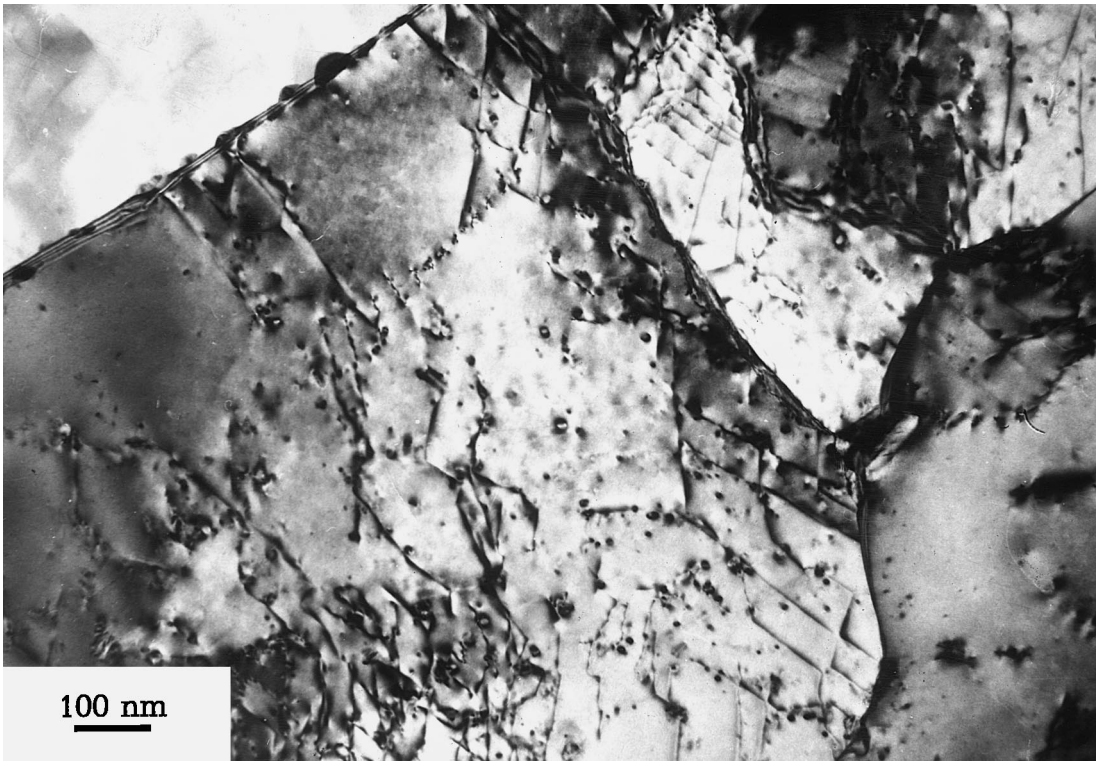

Fig. 6. Radiation defects in irradiated RPVS: ''black dots'' and dislocation loops (bright field image, $F = 6.5 \cdot 10^{23}$ n/m^2),

all visible radiation defects are dislocation loops. In addition, it should be noted that dislocation loops with zero contrast line are glissile dislocation loops. Under the same conditions, the sizes and density of radiation defects grow with increase in fast neutron fluence. The density of radiation defects does not exceed 10^{16} cm^{-3} at fast neutron fluences typical of WWER-440 type reactors.

Irradiation induces considerable increase in disk-shaped precipitate densities (Table 3). Such precipitates are ≈1–2 nm thick with average diameter $\geqslant 20$ nm in initial state and ≈10 nm after irradiation. Fig. 7 illustrates typical histograms of disk-shaped precipitate quantities versus the sizes (diameters) for the steels (surveillance samples) being in various states. These histograms confirm that irradiation induces the formation of a new population of disk-shaped precipitates possessing small sizes. Due to this fact their average sizes are decreasing whereas the density significantly increases (Table 3). The analysis of ellipticity changes of the precipitate images with specimen tilting has shown that the disk-shaped precipitates are located on planes of {1 0 0} type. The following fact is also noted: in addition to the formation of disk-shaped precipitates through the grain volumes, often the precipitates form chains along the grain boundaries (Fig. 8). As shown in [17], the disk-shaped precipitates are vanadium carbides. Their density in real RPVS operating conditions can reach ≈ (5–6) 10^{16} cm^{-3} compared to values in initial state of ≈(0.5–0.8) 10^{15} cm^{-3}.

In addition, irradiation of RPVS also induces the formation of rounded precipitates of quite small sizes: ≈2–3 nm (Fig. 9 and Table 3) [3]. Such precipitates are homogeneously distributed throughout the metal grain volumes. Their density in the considered irradiation conditions reaches $\approx 2 \times 10^{18}$ cm^{-3} (Table 3). As shown in [17], they are copper-enriched precipitates (for more details see Section 4).

2. Recovery annealing at 470–475°C induces nearly complete disappearance of radiation defects in steels (Table 3). In parallel with it, the reduction in disk-shaped precipitate density proceeds to in excess of one order of magnitude (Table 3). Nevertheless, complete recovery of disk-shaped precipitate density to values corresponding to the initial state, does not take place.

[3] Until 1997, the authors did not have a method permitting direct observation of such small precipitates in RPVS during TEM studies. For this reason, the results of TEM studies accomplished before this period did not involve any data on rounded precipitates.

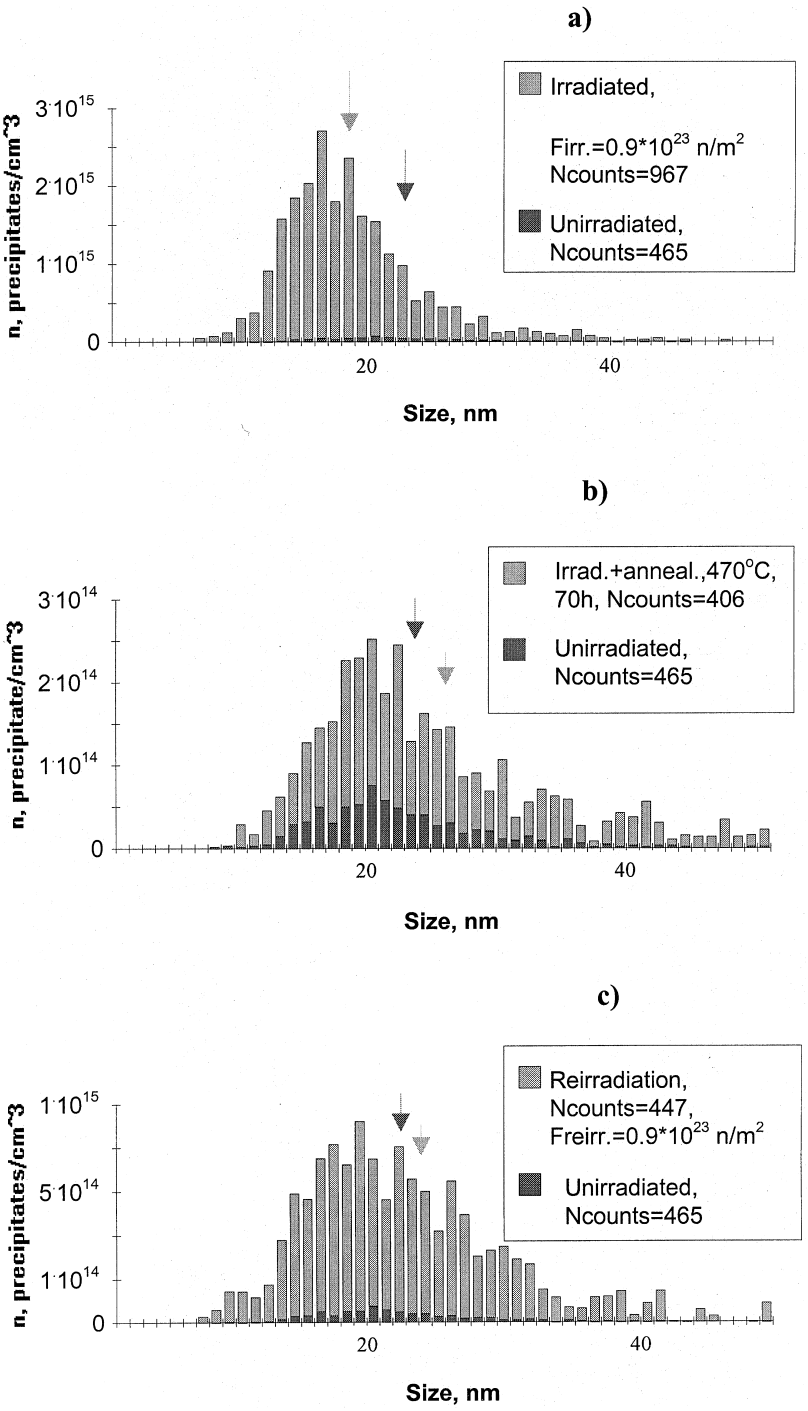

Fig. 7. Size distribution of disk-shaped precipitates for surveillance samples which have undergone: (a) irradiation ($F = 0.9 \cdot 10^{23}$ n/m^2); (b) irradiation and annealing 470°C, 70 h; (c) re-irradiation ($F = 0.9 \cdot 10^{23}$ n/m^2).

Annealing results in a significant change in distribution of disk-shaped precipitates versus the sizes (Fig. 7b). Obviously, the character of such changes depends on neutron fluence accumulated during the steel irradiation. Recovery annealing at 470–475°C causes significant reduction in rounded precipitate density (more than ≈20–

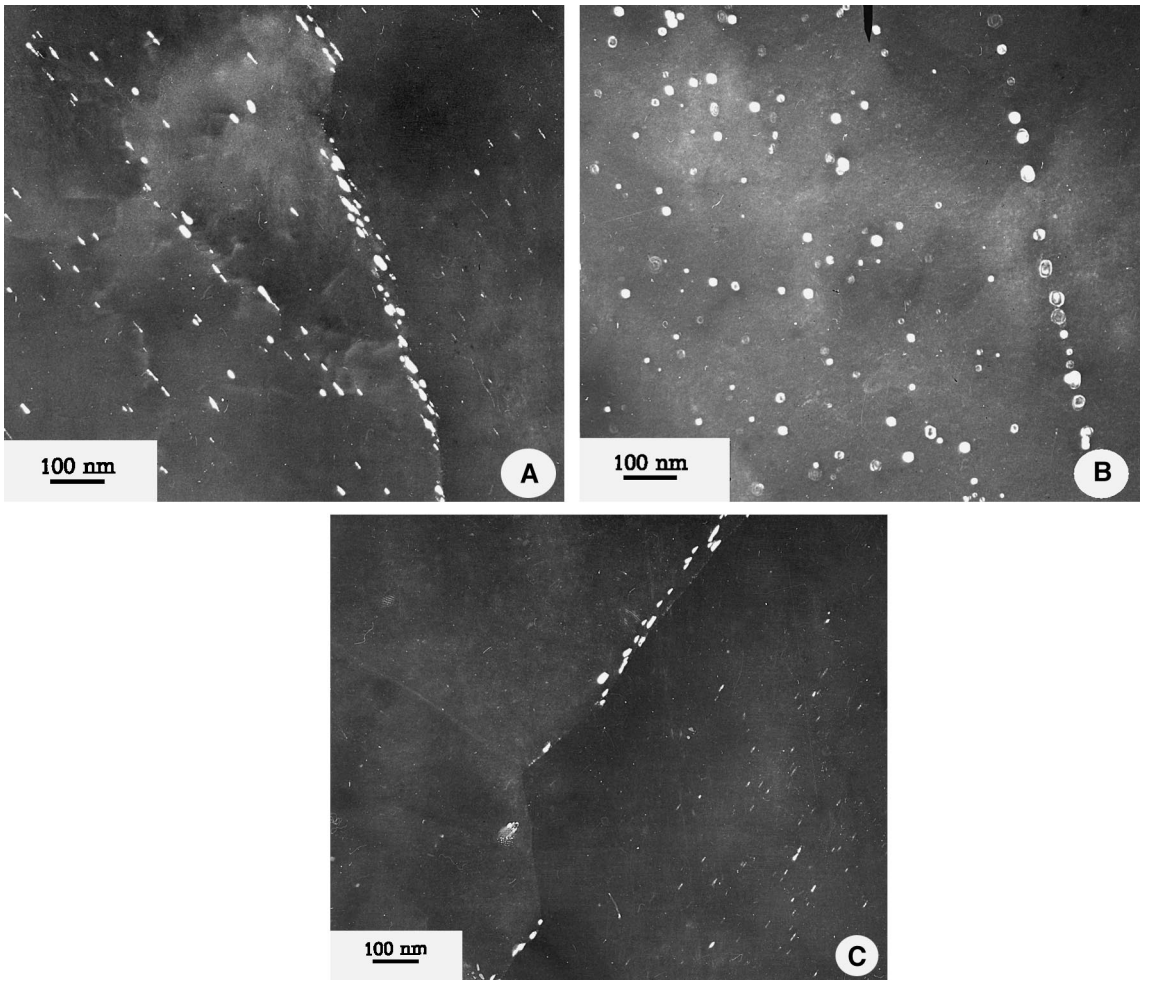

Fig. 8. Disk-shaped precipitates in the body and on the grain-boundary of re-irradiated surveillance samples from weld metal (dark field images, $F = 0.9 \cdot 10^{23}$ n/m^2): (A) side view; (B) front view; (C) irregular disk-shaped precipitate distribution on the grain boundaries.

40 times), and some increase in their average sizes [4] (Table 3).

3. Recovery annealing at ≈560°C causes an even stronger reduction in the density of disk-shaped precipitates (Table 3), but complete recovery of their density (to the values characteristic of unirradiated steels) is not observed. Such annealing leads to more significant changes in size distribution of disk-shaped precipitates as compared with annealing at 470–475°C. As a result, their average size increases to values exceeding average sizes of disk-shaped precipitates in unirradiated steels (Table 3). At the same time, annealing at 560°C induces even more significant reduction in density of rounded precipitates in comparison with annealing at 470–475°C (Table 3).

4. Re-irradiation of steels (after initial irradiation and recovery annealing at 470–475°C) induces the appearance of radiation defects – dislocation loops. However, their density after re-irradiation is somewhat lower, than after initial irradiation (Table 3). At the same time, re-irradiation induces the formation of new populations of disk-shaped and rounded precipitates (Table 3, Fig. 10). It should be mentioned that their density does not reach the values observed after initial irradiation (Table 3). Average sizes of both precipitate types exceed only slightly their average sizes after initial irradiation (Table 3).

[4] Until the present time, the authors have not been successful in seeking rounded precipitates in unirradiated steels, but perhaps this is due to small sizes (<2 nm) and low density of rounded precipitates in the state prior to steel irradiation.

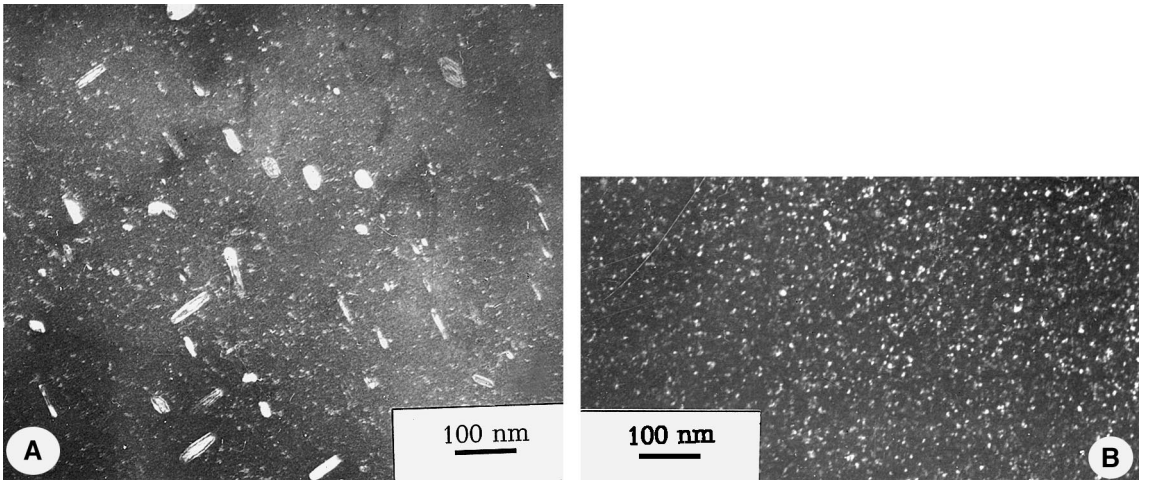

Fig. 9. Precipitates in surveillance samples from weld metal (dark field image): (A) rounded and disk-shaped precipitates in irradiated specimen ($F = 0.9 \cdot 10^{23}$ n/m^2); (B) rounded precipitates in re-irradiated specimen ($F = 0.9 \cdot 10^{23}$ n/m^2).

3.3. Grain-boundary chemical compositions determined by Auger-electron spectroscopy and SIMS

Fig. 11 illustrates a typical Auger-electron spectrum obtained from a fracture surface in the region of intergranular fracture; the specimen was taken from the unirradiated cover of a research reactor, steel 25Kh3NM. This reactor was operating during ≈60 000 h. It can be seen that the grain boundaries are enriched with phosphorus: the ratio of amplitudes of phosphorus to iron

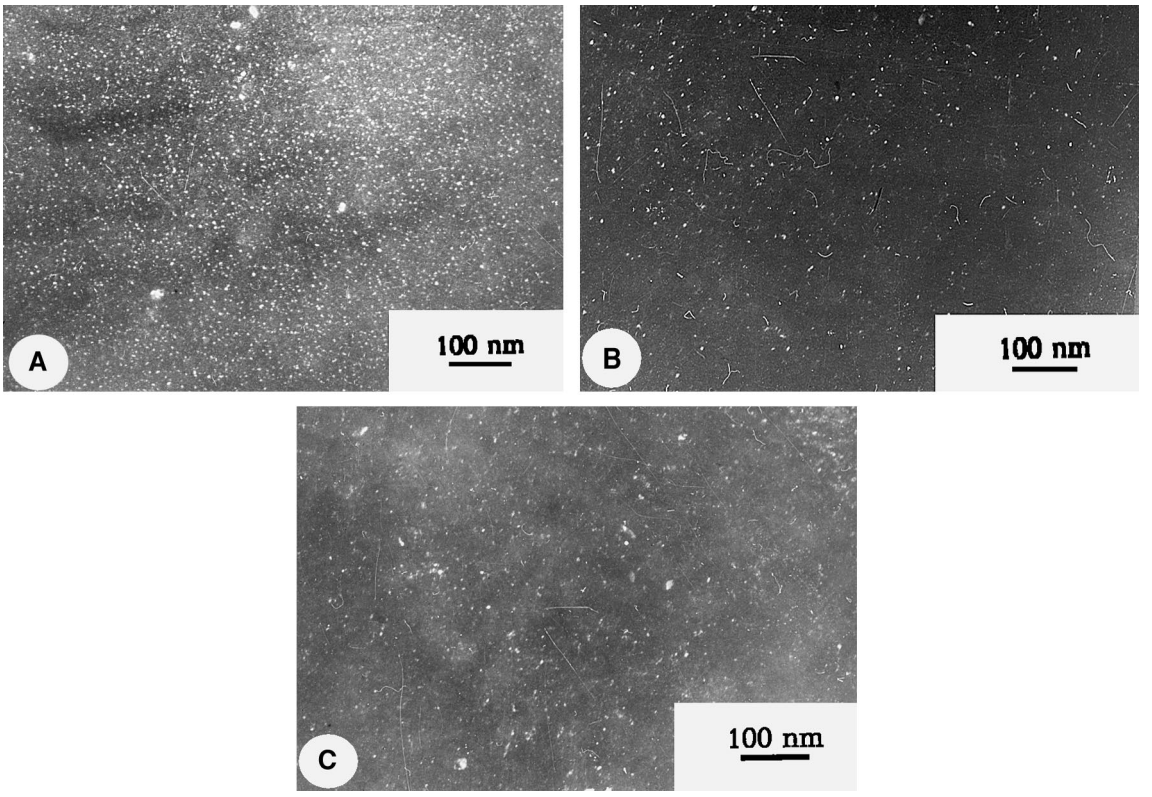

Fig. 10. Rounded precipitates in weld metal (dark field images), which has undergone: (A) re-irradiation ($F = 0.5 \cdot 10^{23}$ n/m^2); (B) re-irradiation and annealing 475°C – 150 h; (C) re-irradiation and annealing 560°C – 2 h.

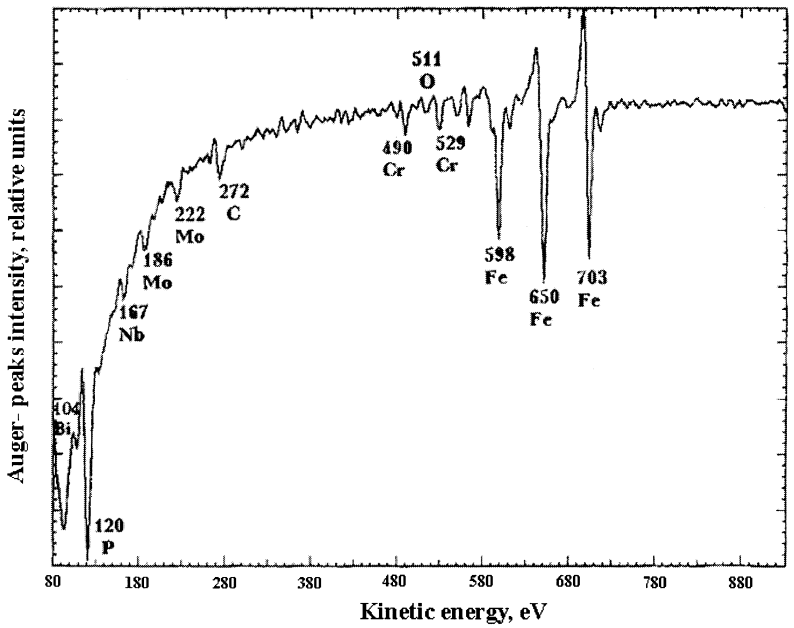

Fig. 11. Auger-electron spectrum of grain-boundary surface (unirradiated base metal from experimental PWR (P = 0.018%wt), heated 60 000 h).

Auger-electron peaks I_P/I_{Fe} is 0.8. Besides, the alloying elements – Nb, Mo, Cr, C – for this steel are represented with the corresponding components in Auger spectrum. Also, the traces of Bi impurity are visible.

Fig. 12 demonstrates the change in the ratio of Auger-electron peak intensities for phosphorus and iron I_P/I_{Fe} due to etching of the specimen fractures by argon ions. It can be seen that with increase in etching time that corresponds to increasing distance from the grain boundaries, the ratio of Auger-electron peak intensities drops to the phosphorus concentration characteristic of the grain body.

Similar results have been obtained using SIMS for irradiated specimens made from WWER-440 pressure vessel produced from steel 15Kh2MFA. Fig. 13 illustrates the distribution of Fe and P in the region of intergranular fracture as a function of increasing distance from grain-boundary. In the present case the fact of

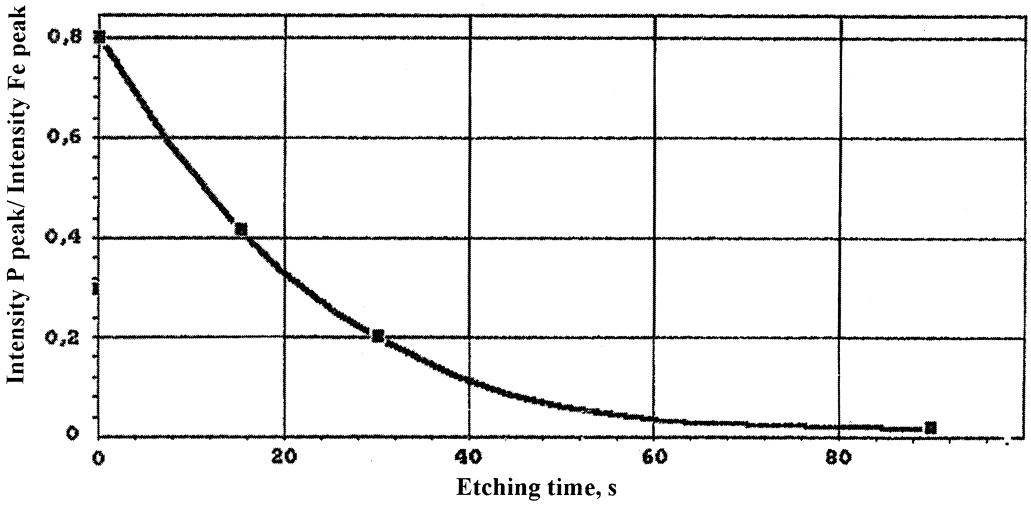

Fig. 12. The change in phosphorus to iron amplitudes I_P/I_{Fe} for Auger-electron peaks resulting from etching of the specimen fractures by argon ions (unirradiated base metal from experimental PWR (P = 0.018%wt) heated 60,000 h).

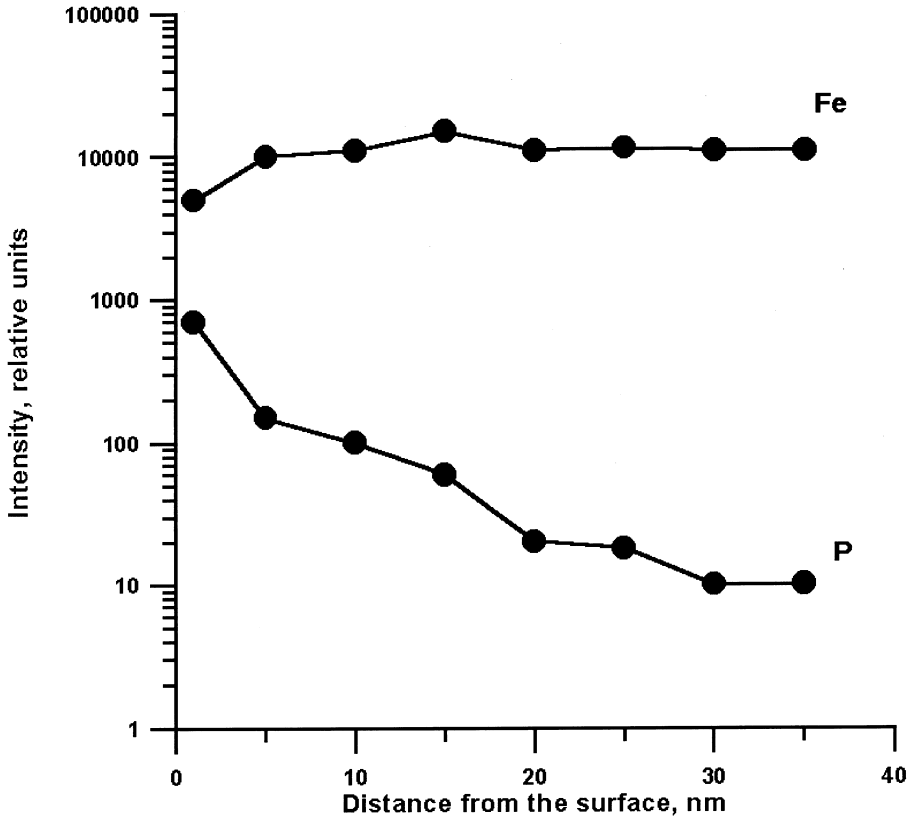

Fig. 13. Chemical composition of irradiated Charpy specimens examined within intergranular fracture regions (base metal, $F = 9.2 \cdot 10^{23}$ n/m^2, P = 0.017%wt).

enrichment of grain boundaries with phosphorus is valid. Thus, within the regions of specimen fractures with intergranular character of fracture, the grain-boundary phosphorus segregation has been observed (resulting from both irradiation and long-term heat exposure).

4. Discussion

The data obtained show that irradiation of Russian RPVS (first of all, weld metal) induces the following structural changes:

1. The appearance of radiation defects – dislocation loops.
2. Significant increase in disk-shaped precipitate densities and appearance of great number of rounded precipitates. Obviously, the former are vanadium carbides, whereas the latter are copper-enriched precipitates.
3. Formation of grain-boundary and intragranular segregation of impurities (primarily, phosphorus).

In [12] the different mechanisms were discussed in detail and their relative contribution to RE occurring in RPVS was evaluated (i.e., their contribution to the DBTT shift measured during impact testing). It was shown that RE is primarily determined by intragranular phosphorus segregation and to a smaller extent by radiation hardening induced by various precipitates and radiation defects. The contribution from grain-boundary phosphorus segregation to RE proceeding in RPVS does not exceed 10–20%.

The data obtained in the present study and involving complex microstructural and fractographic investigations allow to elucidate the way in which the mechanisms (radiation hardening, intragranular and intergranular segregation) are realized and how they lead to RE in RPVS.

It is well known that in steels possessing a BCC crystal lattice, the appearance of regions with brittle intergranular fracture is usually determined by impurity (primarily, phosphorus) segregation to grain boundaries. Direct experimental studies of impurity distributions in fractures of irradiated specimens, accomplished for the regions with intergranular fracture type (using SIMS and Auger-electron spectroscopy) confirm the fact of grain-boundary phosphorus segregation there [18]. Irradiation temperatures (≈250–290°C) providing the

appearance of grain-boundary phosphorus segregation in RPVS, are significantly lower than the temperatures characteristic of temper brittleness (≈400–500°C) [19]. Unfortunately, practically all experimental data on temper brittleness were obtained with time periods of exposure not exceeding 10 000–20 000 h [19]. The shortage of data does not allow to unambiguously separate the radiation component during formation of grain-boundary phosphorus segregation in RPVS irradiated at operating temperatures ≈250–300°C and duration of exposure ≈200 000–300 000 h. The indicated time interval approximately corresponds to RPV lifetime. It is known that the affinity of phosphorus to grain boundaries in steels at temperatures $\geqslant$ 600–650°C is zero and steadily increases with temperature decreasing under these values [19]. At low temperatures the process of grain-boundary phosphorus segregation is governed exclusively by kinetic factor, since the stationary phosphorus level in grain-boundary segregation is steadily increasing with decrease in temperature (<600–650°C) [19]. Therefore, prolongation of heating exposure (by one order of magnitude and more if compared with the main body of experimental data obtained for temper brittleness) can considerably change the shape of temperature dependencies of grain-boundary phosphorus segregation evolution within the region of reduced temperatures.

Isolated experimental data show that long-term (≈60 000 h) heating exposure of RPVS at ≈270°C without irradiation induces phosphorus segregation to grain boundaries. Moreover, the fraction of the regions with brittle intergranular fracture type in Charpy specimens can reach 65% (Table 2, lines 1,2). For Charpy specimens made from the same steel which had undergone irradiation – as a part of RPV – to different neutron fluences (1.6×10^{23} – $5.05 \times 10^{23} m^{-2}$) at ≈270°C and also testing, the fraction of the regions with brittle intergranular fracture type constitutes ≈65–70% (Table 2, lines 4–8). These data demonstrate that phosphorus segregation to grain boundaries in RPVS, proceeding during ≈60 000 h (which is 3–10 times longer than usual duration of surveillance samples irradiation), chiefly are not governed by the radiation effects (irradiation), but by the parameters of heating exposure, similar to the process of temper brittleness evolution.

It should be kept in mind that the overwhelming portion of the data on RE in RPVS was obtained within the framework of surveillance sample (SS) examinations. Irradiation of SS is more or less accelerated if compared with real RPV operating conditions. The duration of SS irradiation examined until the present time does not exceed ≈20 000–30 000 h. The available experimental data do not permit to evaluate the degree of temper brittleness evolution in RPVS caused of heating exposure at operating temperatures for the above time intervals. But it is reasonable to suppose that the level of grain-boundary phosphorus segregation by accelerated irradiation of SS would be found out lower than in similar steels of RPV still being in operation, when they will be taken out of service (under the same other conditions – i.e., equality of temperatures and fast neutron fluences). Thus, it can be predicted that phosphorus level in grain-boundary segregation for SS will differ from equilibrium (stationary) level for the temperature considered – to higher extent than phosphorus level in grain-boundary segregation for the same steel taken from RPV when it will be taken out of service. The reason of this predicted difference is the considerable difference in duration of heating exposure during irradiation. By all the above reasons, the contribution to grain-boundary phosphorus segregation in steels undergoing accelerated irradiation from pure radiation effects (for instance, radiation-induced diffusion) would be higher than in similar steels irradiated in operating RPV.

It should be mentioned that in studies devoted to temper brittleness in steels, enhanced grain-boundary phosphorus segregation due to increase in nickel content was noted [19]. In this connection, one can suppose that in RPVS with heightened nickel content (e.g., in WWER-1000 RPV materials) the contribution from the temper brittleness mechanism to final phenomenon of grain boundary phosphorus segregation caused of irradiation would be higher.

The analysis of fractographic data confirms that the decrease in fraction of the regions with brittle intergranular fracture type in irradiated specimens and also specimens, which have undergone temper embrittlement heat tratment, is observed at the same temperatures ($\geqslant$ 560°C). Therefore, it can be deduced that the decay of grain-boundary phosphorus segregation resulting from annealing is proceeding at the same temperatures independent of the way of their formation, whether by temper embrittlement or by irradiation. This situation looks quite natural, since the formation and decay of grain-boundary phosphorus segregation proceeding in steel are reversible relative to temperature and can be described analytically using state functions (potential functions) [19]. By this reason, the prehistory of grain-boundary phosphorus segregation does not have to influence the regularities of their decay in the process of recovery annealing. By the above reasons, recovery annealing at ≈450–500°C applied to irradiated RPVS does not induce any reduction in the fraction of brittle intergranular component in specimen fractures (Table 2, lines 22,23, 28,29, 40,41, 46–48). Respectively, this annealing does not induce the recovery of those parts of RE, which is caused by grain-boundary phosphorus segregation. And what is more, annealing at such temperatures can induce the increase in the level of grain-boundary phosphorus segregation, if its duration is long enough.

The analysis of the data obtained displays that in similar materials (base or weld metal), at comparable irradiation conditions, an increase in phosphorus concentration induces the increase in the fraction of the regions with brittle intergranular fracture type in Charpy specimens. However, the quantity relation between phosphorus concentration and the number of brittle intergranular fracture regions is rather complicated. For example, in full-size Charpy specimens made from base metal, where phosphorus content is a few times lower than in weld metal, the fraction of the regions with brittle intergranular fracture type after irradiation in comparable conditions is significantly higher (see Section 3). Apparently, this is due to variations in microstructure of the materials considered.

In agreement with the data from [20], the following probable reason of stronger inclination of Russian grade irradiated full-size Charpy specimens made from base metal to brittle intergranular fracture in compare with Russian grade irradiated full-size Charpy specimens made from weld metal may be pointed out. Metallographic studies have shown that microstructure of base metal is homogeneous and consists of tempered bainite. In contrast with base metal, the bodies of weld metal grains consist of tempered bainite whereas grain boundaries of prior austenitic grains are decorated by globular alpha-ferrite (Fig. 14). The preferential intergranular fracture in Charpy specimens is passing just through these high-angle grain boundaries of prior austenite. Alloying of steels with Mo and Mn induces abrupt decrease in phosphorus solubility in alpha-ferrite [20] and, respectively, can induce the reduction of phosphorus segregation level along the weld boundaries. The validity of this reason is confirmed by the fact that the appearance of brittle intergranular fracture in full-size Charpy specimens from American grade steel is equiprobable as due to base or weld metal specimens that have the same homogeneous structure of tempered bainite along the section of the former austenitic grains [13]. However, the appearance of the area with brittle intergranular fracture in irradiated sub-size Charpy specimens of Russian grade weld metal is quite probable due to peculiarities of stress deformation state caused by impact tests.

First of all, it should be emphasized that the most convincing direct experimental fact, pointing to the appearance of intragranular phosphorus segregation as a result of irradiation, is the appearance – in the fractures of the corresponding Charpy specimens – of the regions with ductile intergranular fracture type (Table 2). In compliance with [12,21], the appearance of such regions in fractures may occur only when grain boundaries are decorated with precipitates, and, moreover, at the interface boundaries of these precipitates, phosphorus segregation is proceeding in the process of heat treatment or irradiation. In general, such precipitates could be present at the grain boundaries in initial state as well and/or appear as a result of irradiation or heat treatment.

The fact that ductile intergranular fracture is observed at impact testing temperature that belongs to the US regime, indicates the low level of the values of the stress of tearing in the region of interface boundaries of these precipitates. Besides, this fact confirms that at the indicated interface boundaries, the level of the stress of tearing is lower, than at those boundaries of the matrix grains, where usual grain-boundary phosphorus segregation had been proceeding. This conclusion follows

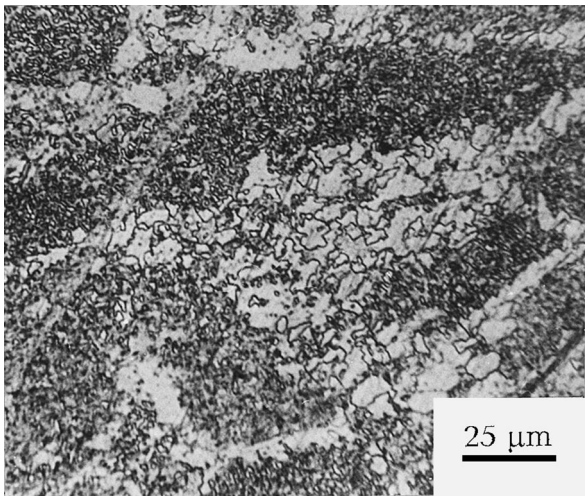

Fig. 14. Typical microstructure of WWER-440 weld metal. The globular inclusions of alpha-ferrite decorate the grain boundaries of prior austenitic grains.

from the fact that at impact testing temperatures in the US regime, brittle intergranular fracture is practically absent (Table 2).

The reasons of the distinction in the values of the stress of tearing at interface boundaries of precipitates and boundaries of the matrix grains by appearance of phosphorus segregation at them are not clear at the present moment. Probably, they are related to peculiarities in structure of interface boundaries and also with the distinctions in the level of phosphorus segregation on them.

Fracture character in the regions with ductile intergranular fracture points to the fact that the average distance between precipitates (at interface boundaries of which the phosphorus segregation had taken place), decorating the corresponding boundaries of the matrix grains, should not exceed ≈1–5 μm. This value corresponds to the average distance between the centers of the adjacent dimples on the areas with ductile intergranular fracture. TEM studies have shown that in irradiated weld metal the indicated requirement can be satisfied only for disk-shaped and rounded precipitates of rather high density. It is worth mentioning that the decoration of the regions of matrix grain boundaries with precipitates is observed only infrequently [5] (Fig. 8C). As shown above, the precipitates of such type arise preferentially inside the grain body. Obviously, when the interface boundaries of some precipitates possess an affinity for phosphorus, then under the same other conditions, phosphorus segregation to them will be proceeding independent of their location either inside the body or at the boundary of the matrix grains. It should be noted that in [22] the precipitates inclined to phosphorus segregation at their interface boundaries due to heating exposure were registered also inside the body of the matrix grains in addition to location along the boundaries. The fact of the appearance of the regions with ductile intergranular fracture type in the fractures, by itself, is pointing to the fact that the tearing along precipitate interface boundaries, decorating the boundaries of the matrix grains, occurs at a little bit lower level of stresses, than along interface boundaries of the same precipitates, situated inside the matrix grains.

Separate experimental studies using APFIM, confirm that the appearance of copper-enriched precipitates resulting from RPVS irradiation, is accompanied by their enrichment with phosphorus as well [23]. Thus, it is reasonably to suppose that phosphorus segregates also to interface boundaries of copper-enriched precipitates. As well, the above considerations allow to suppose that in weld metal, in addition to appearance of disk-shaped and rounded precipitates and significant increase in their density, irradiation also induces phosphorus segregation to their interface boundaries or, in the other words, intragranular segregation. One cannot exclude that phosphorus segregation may be proceeding at interface boundaries of other precipitate types. But in weld metal, the density of all other precipitates is much lower than the above discussed one, and practically is not changing under irradiation.

The data in [22] demonstrate that the processes of phosphorus segregation resulting from steel tempering at precipitate interface boundaries, are reversible relative to the temperature (which is quite similar to well known grain-boundary phosphorus segregation). It is worth noting that the temperatures of their formation, stability and decay, practically, do not differ from the corresponding temperatures for grain-boundary phosphorus segregation. For example, the temperatures at the moment of the beginning of the decay of phosphorus segregation at the interface boundaries are above 525°C [21,22]. It is pointed out in [12] that the disappearance of intragranular phosphorus segregation (in contrast with grain-boundary phosphorus segregation) may occur at lower annealing temperatures, if this is not caused of segregation dissolution, but due to the dissolution of the precipitates themselves. The results of TEM studies (Table 3) demonstrate that recovery annealing at 470–475°C applied to irradiated weld metal induce a decrease in density of disk-shaped and rounded precipitates by more than one order of magnitude. This circumstance allows to confirm that recovery annealing at this temperature ought to lead to higher degree of the recovery of changed properties related to radiation-induced intragranular phosphorus segregation. The increase in annealing temperature to 560°C induces even stronger decrease in density of precipitates of both types (Table 3) and increase in the degree of recovery of DBTT.

The results of TEM studies (Table 3) show that recovery annealing at 470–475°C applied to irradiated weld metal induced practically complete disappearance of radiation defects – dislocation loops. This circumstance in combination with the above ones, defines high degree (≈90%) of radiation-induced hardening recovery and the decrease in steel ductility accompanying it (see [12]), which is proceeding after recovery annealing already at 470–475°C. These considerations become quite transparent, if one takes into account that the reason of hardening occurring in the steels as a result of irradiation is the formation of radiation defects, increase in density of disk-shaped and rounded precipitates. As known [19,21,22], phosphorus segregation does not deliver any contribution to hardening.

Comparison of experimental data obtained in the present study with published data on grain-boundary and intragranular phosphorus segregation in steels are

[5] A small fraction of the ductile intergranular fracture on the fracture surface is due to infrequent grain boundary decoration with the precipitates.

pointing to deep analogy between these two phenomena. First of all, they both are reversible relative to the temperature, and also the temperatures characteristic of the appearance or decay of both types of segregation are close. In this connection (similarly to the above considerations concerning grain-boundary phosphorus segregation), it is evident, that RPVS operating temperatures are significantly lower than the temperatures of phosphorus segregation in them. But limited data on the appearance of intragranular phosphorus segregation in steels were obtained in the process of thermal aging of duration not exceeding ≈20 000 h [22]. Approximately, this corresponds to typical duration of SS irradiation and is much less than RPV lifetime.

The deficiency of the data does not permit to reveal unambiguously the radiation component in the process of phosphorus segregation evolution in RPVS at operating temperatures ≈250–300°C. But, similar to the above considerations concerning grain-boundary phosphorus segregation, one can suppose the following. The level of phosphorus segregation at precipitate interface boundaries resulting from accelerated irradiation of SS would be found out to be lower, than in similar steels of operating reactors at the moment when they will be taken out of service (under the same other conditions, i.e., equal irradiation temperatures and fast neutron fluences). As pointed out above, for formation of intragranular phosphorus segregation, in addition to phosphorus, the precipitates are a necessary requirement, which possess propensity for phosphorus segregation to their interface boundaries. Such precipitates could be present inside RPVS before irradiation. But considerably more of such precipitates (disk-shaped and rounded) are created in the process of irradiation. Primarily, their formation is the consequence of the known fact that during RPVS production, in the steel matrix, the concentrations of some impurity elements (for instance, copper) significantly exceeding their equilibrium solubility values characteristic of the reactor operating temperatures. Therefore, the duration of thermal exposure in the process of RPVS exploiting (and not just irradiation) can influence on the degree of the approach of concentrations of these impurities to equilibrium values.

All the above circumstances point to the fact that accelerated irradiation of SS and irradiation of the same steels during RPV operation (at the same temperatures and to the same neutron fluences) are accompanied by different structural changes. It should be pointed out here that structural changes in steels irradiated in RPV have to be stronger than similar changes occurring in SS (the level of grain-boundary and intragranular impurity segregation and also the density of disk-shaped and rounded precipitates are higher (Table 3)). Finally, the components of RE, which are associated with grain-boundary and intragranular phosphorus segregation have to be larger in the steels irradiated in RPV. Consequently, the long duration of thermal exposure can be the principal factor inducing so-called phenomenon of "small fluxes". As well, it is evident that the above considerations are applicable only if the values of neutron fluences do not exceed a definite limit. At high enough values of neutron fluences due to exhaustion of phosphorus, copper etc. contents in the matrix, the principal contribution to RE can be delivered by radiation defects (i.e., because of reduction in steel ductility), then the above considerations would lose their importance. Consequently, the phenomenon of small fluxes has to manifest stronger by irradiation of RPVS with higher phosphorus content, copper and, probably, some other elements composing the precipitates, forming in the process of irradiation.

The results detailed in Section 3 demonstrate that during weld metal re-irradiation (which primarily had undergone recovery annealing at 470–475°C after irradiation) in absolutely identical conditions, the rate of structural changes is significantly reduced. The density of radiation defects, disk-shaped and rounded precipitates after re-irradiation is noticeably lower, than after initial irradiation (Table 3). The most probable reason of this phenomenon is incomplete recovery of radiation-induced structural changes after recovery annealing at 470–475°C. First of all, this is valid for disk-shaped and rounded precipitates, but also for grain-boundary phosphorus segregation and phosphorus segregation to interface boundaries of the above precipitates, which have preserved after recovery annealing.

Thus, RPVS microstructure in the initial state (before irradiation) differs significantly from microstructure of the same materials after recovery annealing at temperatures not exceeding 500°C. As known, the dose dependencies of the property changes and characteristics of the material structures in the process of irradiation are, as a rule, the curves with the exponent not exceeding 1. That is why, by incomplete annealing of radiation-induced structural changes in steels, the parameters of their structure may correspond to some intermediate point at the corresponding dose dependencies. The further is this point from the origin of coordinates, the less is the value of the corresponding derivative. Accordingly, the less is the rate of the property changes occurring in the material structure and resulting from re-irradiation in this case. The available experimental data qualitatively confirm the correctness of this reasoning. For instance, it was demonstrated in a series of examples, that the lower the temperature of recovery annealing applied to irradiated RPVS, the lower the rate of changes in their properties resulting from re-irradiation [24].

However, these considerations do not exhaust all probable causes of the distinctions in the rate of changes in structure and material properties resulting from re-

irradiation after recovery annealing as compared with initial irradiation. It was pointed out above that some portion of precipitates induced by irradiation (rounded precipitates) are enriched with copper. Interface boundaries of disk-shaped, rounded and, probably, some other precipitate types are enriched with phosphorus after irradiation. In addition, irradiation leads to grain-boundary phosphorus segregation. The circumstances enumerated above could lead to reduction in the contents of copper and phosphorus impurities (and, probably, some other elements) and, besides, they could lead to changes in the proportions among their concentrations in steel matrix resulted from irradiation.

Recovery annealing at 470–475°C does not induce recovery of density and sizes of disk-shaped and rounded precipitates back to initial values (Table 3). Due to this fact, phosphorus segregation is preserved at interface boundaries of those precipitates that have not dissolved during annealing. Besides, during such annealing, grain-boundary phosphorus segregation are not dissolving as well. Therefore, the recovery annealing at 470–475°C cannot lead to recovery of concentrations and proportion between copper and phosphorus concentrations in the steel matrix to initial values. Due to the fact that these impurities strongly influence the rate (coefficient) of RE in RPVS [25], the reduction in their concentration in the matrix might be the extra reason of the observed rate of structural changes and steel properties resulting from re-irradiation. As well, it can be deduced from the above that dose dependencies of RE, obtained for RPVS at initial irradiation have to demonstrate significant discrepancies as compared with dose dependencies corresponding to re-irradiation of the same steels, which have undergone recovery annealing at $\leqslant$ 470–475°C. These discrepancies have to manifest in higher degree in accordance with:

- reduction in the temperature of recovery annealing (at least within the range $\approx$340–475°C),
- increase in neutron fluences and also duration of initial irradiation.

The above factors facilitate the reinforcements of discrepancies in concentration and proportion between copper and phosphorus impurity concentrations in the matrix of the same steel in the states preceding initial- and re-irradiation.

5. Conclusions

The complex studies of RPVS structure before and after irradiation and also after recovery annealing and re-irradiation allow to make the following conclusions:

1. Irradiation of RPVS induces the combination of structural changes, which involve: formation of radiation defects, phase transformations with formation of a few types of superfine, dispersed precipitates, intragranular and grain-boundary impurity segregation (primarily, phosphorus).
2. Structural changes due to irradiation lead to the changes in fracture character of the specimens made from irradiated RPVS resulting from impact tests and the increase in the DBTT, i.e., radiation embrittlement occurring in steels. Moreover, the fracture surface in unirradiated RPVS specimens is transcrystalline type. After irradiation the fracture type is mixed: a valuable quantity of the regions with ductile intergranular or brittle intergranular fracture surface types may appear in the fractures.
3. Recovery annealing applied to irradiated RPVS at temperature not exceeding 475°C (i.e., annealing temperatures used for prolongation of RPV lifetime) does not provide complete recovery of radiation-induced structural changes. Such annealing facilitates considerable, but not complete recovery of radiation-induced precipitate and intragranular phosphorus segregation densities. However, they do not induce the reduction of grain-boundary phosphorus segregation and can facilitate their reinforcements.
4. Structural changes resulting from recovery annealing applied to RPVS lead to significant reduction in the fraction of the regions of ductile intergranular fracture type and do not change (or magnifies the fraction of the regions of brittle intergranular fracture type in fractures of Charpy specimens). Structural changes as well as Charpy specimen fracture surface changes lead to significant recovery of the DBTT observed for RPVS that have undergone recovery annealing.
5. Re-irradiation applied to RPVS (in comparable conditions) is accompanied by essentially lower rate of structural changes as compared with initial irradiation and also lower rate of radiation embrittlement.
6. The observed experimental phenomena concerning structural and fracture type changes in Charpy specimens made from RPVS in different states permit to explain qualitatively the features of radiation embrittlement occurring in them and resulting from initial- and re-irradiation. But this is necessary to continue the studies in this direction.

Acknowledgements

The authors render their deep gratitude to P.A. Platonov, A.M. Kryukov, Ye.A. Krasikov, Yu.N. Korolev, Yu.A. Nikolaev, V.N. Nevzorov, A.Yu. Biryukov, D.Yu. Yerak for many valuable advice and the help in their studies.

References

[1] I. Churchman, A.H. Mogford, V. Cottrell, Philos. Mag. 2 (1957) 1271.

[2] J.R. Hawthorne, in: C.L. Briant, S.K. Benerji (Eds.), Treatise on Materials Science and Technology, Embrittlement of Engineering Alloys, vol. 25, ch. 10, Academic Press, NY, 1983.

[3] N.N. Alexeyenko, A.D. Amaev, I.V. Gorynin, V.A. Nikolaev, Irradiation Damage of Pressured Water Reactor Vessel Steels, Energoatomizdat, Moscow, 1981.

[4] R.B. Jones, J.T. Buswell, in: Dimensional Stability and Mechanical Behaviour of Irradiated Metals and Alloys, Proceedings of BNES Conference, Brighton, 1983, London, vol. 2, 1984, p. l05.

[5] M.K. Miller, M.G. Burke, J. Nucl. Mater. 195 (1992) 68.

[6] G. Brauer, F. Eichhorn, F. Frisius, R. Kampman, in: A.S. Kumar, D.S. Gelles, R.K. Nanstad, E.A. Little (Eds.), Effect of Radiation on Materials, ASTM STP 1175, American Society for Testing and Materials, Philadelphia, PA, 1993, pp. 503–515.

[7] T.J. Williams, W.J. Phythian, in: D.S. Gelles, R.K. Nanstad, A.S. Kumar, E.A. Little (Eds.), Effect of Radiation on Materials, ASTM STP 1270, American Society for Testing and Materials, 1996, pp. 191–205.

[8] M.K. Miller, S.S. Brenner, Res. Mech. 10 (3) (1984) l61.

[9] M.K. Miller, R. Jayaram, P.J. Othen, G. Brauer, Appl. Surf. Sci. 76&77 (1994) 242.

[10] G. Brauer, L. Liszkay, R. Krause, Nucl. Eng. Design 127 (1991) 47.

[11] G.R. Odette, Scripta Metall. 17 (1983) 1183.

[12] B.A. Gurovich, E.A. Kuleshova, Yu.A. Nikolaev, Ya.l. Shtrombakh, J. Nucl. Mater. 246 (1997) 91.

[13] B.A. Gurovich, E.A. Kuleshova, O.V. Lavrenchuk, J. Nucl. Mater. 228 (1996) 330.

[14] S.A. Saltykov, Stereometric Metallography, Metallurgiya, Moscow, 1976.

[15] P.M. Kelly, A. Jostsons, R.G. Blake, J.G. Napier, Phys. Status Solidi A 31 (1975) 771.

[16] B.C. Edwards, B.L. Eyre, G. Gage, Acta Metall. 28 (1980) 335–356.

[17] M.K. Miller, M.G. Burke, in: N.H. Packan, R.E. Stoller, A.S. Kumar (Eds.), Effect of Radiation on Materials, ASTM STP 1046, American Society for Testing and Materials, Philadelphia, PA, 1990, p. 120.

[18] Yu.A. Nikolaev, A.V. Nikolaeva, O.O Zabusov, B.A. Gurovich, E.A. Kuleshova, A.A. Chemobaeva, Fiz. Metall. Metalloved. (1996) 81–1 .

[19] L.M. Utevsky, E.E. Glikrnan, G.S. Kark, Reverse Temper Embrittlement of Steel and Iron Alloys, Metallurgiya, Moscow, 1985, pp. 10–49.

[20] I.I. Novikov, Theory of Metals Heat Treatment, Metallurgiya, Moscow, 1978, p. 392.

[21] S.G. Druce, Acta Metall. 34 (1986) 219.

[22] J.A. Hudson, S.G. Druce, G. Gage, M. Wall, Theor. Appl. Fracture Mech. 10 (1988) 123.

[23] M.K. Miller, M.G. Burke, in: A.S. Kumar, D.S. Gelles, R.K. Nanstad, E.A. Little (Eds.), Effect of Radiation on Materials, ASTM STP 1175, American Society for Testing and Materials, Philadelphia, PA, 1993, p. 492.

[24] P.A. Platonov, Ya.A. Schtrombakh, A.M. Kryukov, in: A.S. Kumar, D.S. Gelles, R.K. Nanstad, E.A. Little (Eds.), Effect of Radiation on Materials, ASTM STP 1325, American Society for Testing and Materials, 1997, p. 129.

[25] Calculation Standards for Strength of Equipment and Pipes of Nuclear Power Units, PNAE-G-7-002-86, Energoatomizdat, Moscow, 1989.